

Application of a novel lateral force-sensing microindentation method for evaluation of the bond strength of thermal sprayed coatings

H. Zhang*, D.Y. Li

Department of Chemical and Materials Engineering, University of Alberta, Edmonton, Alberta, Canada T6G 2G6

Received 15 March 2004; accepted in revised form 25 June 2004

Available online 17 August 2004

Abstract

A novel lateral force-sensing microindentation method was applied to evaluate the interfacial bond strengths of regularly grained and nanograined $\text{Al}_2\text{O}_3/\text{TiO}_2$ composite coatings. The interfacial bond strength, i.e., the bond between a coating and its substrate (steel), was determined by performing microindentation tests, on a cross section near the interface. By monitoring changes in lateral force during indentation, the critical indentation force at interfacial debonding was determined. The interfacial bond strength was then determined based on this critical indentation force and interfacial stress analysis using the finite element method. The results were compared to those obtained from a pull-off test and showed consistency with them.

© 2004 Published by Elsevier B.V.

Keywords: Interfacial bond strength; Microindentation; Lateral force; Thermal sprayed coating

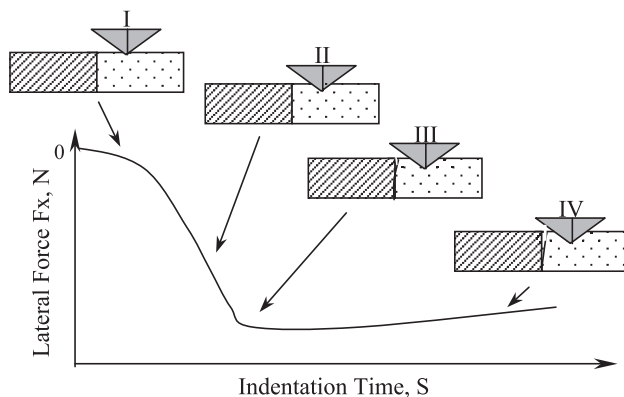
1. Introduction

Evaluation of the interfacial bond strength for coatings has been an important and difficult task in surface engineering. Many testing methods, such as the pull-off test [1,2], bending test [3,4], and peel-off test [5,6], have been employed to evaluate the bond strength. However, these methods only provide average bond strength and test results may not correctly represent the intrinsic bond strength and reflect associated interfacial failure mode [7]. Application of these methods is also limited by other factors. For example, for the pull-off test, the adhesive used to glue a sample to the sample holder is required to have its bond strength higher than that of the interface. It is also difficult to use bending and peel-off tests to evaluate hard and brittle coatings [8]. Scratch testing [9,10] is another technique for evaluating coating's adherence to substrate by moving a small diamond tip over the sample surface under a progressively increasing load. The initia-

tion of interfacial debonding is detected from acoustic emission signals or the local load-displacement curve; the corresponding critical scratching load could thus be determined. However, cracking of coating may also produce acoustic signals or unusual changes on the load-displacement curve, so that the detected failure events may not be always related to debonding of the coating-substrate interface. In addition, the critical scratching load is also affected by the shape of the stylus, coating thickness, mechanical properties of the coating and substrate, etc. These factors make the scratching method only semiquantitative. Microindentation is a promising technique for interfacial bond evaluation. Microindentation may be performed on the cross section of a sample, either directly at interface between coating and substrate [11] or at the substrate near the interface [12], to evaluate the interfacial bond. The length of crack at interface caused by indentation is used to evaluate the interfacial toughness or strength. This method, however, only provides qualitative information on the interfacial bond; furthermore, at this stage, the method cannot be used to determine the initiation of interfacial debonding. There are also other methods for evaluating interfacial bonds, such as the

* Corresponding author. Tel.: +1 780 492 5806; fax: +1 780 492 2881.

E-mail address: hongz@ualberta.ca (H. Zhang).



cavitation test [9] and the laser spallation test [13]. However, these methods are only suitable for specific coatings, and their applications are limited.

Recently, the authors proposed a new method—the lateral force-sensing indentation technique—to evaluate the interfacial bond strength [14,15]. During the test, indentation is performed on the cross section at the substrate side near the interface. Due to the asymmetrical constraint on the indenter tip when the tip is pressed near the interface, the indenter tip bears a non-zero lateral force whose magnitude increases as the indentation force is increased. When interfacial debonding occurs, the constraint from the interface is partially released. As a result, the tip will move in the opposite direction and result in a change in sign of the slope of the lateral force–time curve as Fig. 1 shows. The critical indentation load corresponding to initiation of interfacial debonding can thus be determined. Based on the critical indentation load, the interfacial bond strength can be calculated using the finite-element method in combination with a Quadratic Delamination Criterion [14–16]. In this work, this method was applied to determine interfacial bond strength of a commercial thermal sprayed $\text{Al}_2\text{O}_3/\text{TiO}_2$ coating (Mecto 130) and a nanostructured $\text{Al}_2\text{O}_3/\text{TiO}_2$ coating on a mild carbon steel substrate. The obtained results were compared to results of a pull-off test. It was demonstrated that the lateral force-sensing indentation method was effective for the determination of interfacial bond strength.

2. Experimental method

In this work, interfacial bonds of thermal-sprayed $\text{Al}_2\text{O}_3/\text{TiO}_2$ composite coatings on steel substrate were evaluated. Compositions of the coatings were 87 wt.% Al_2O_3 and 13 wt.% TiO_2 . One type of the coating had regular microstructure of melted splats. The plasma spray condition has been given in Ref. [17]. Another type of coating was deposited using nanocrystalline powders, which was com-

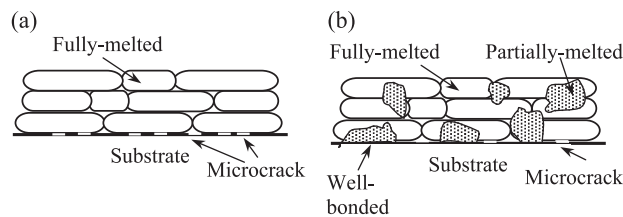


Fig. 2. Schematic illustrations of microstructures of two coatings. (a) Metco130 and (b) nanocoating.

posed of two different parts; one had the microstructure similar to that of Metco130 with fully melted features, and the other had partially melted domains embedded in the melted splats [18]. Details about the fabrication of the $\text{Al}_2\text{O}_3/\text{TiO}_2$ nanocoating as well as microstructures and properties of these two types of coating have been reported in literature [17–19]. A schematic illustration of microstructures of these two coatings is shown in Fig. 2. Both coatings were deposited on a mild carbon steel, which was blasted to remove rust and cleaned [17]. The coated steel was sectioned into 13×12 mm rectangular plates consisting of 3-mm-thick substrate and 100- μm -thick coating. The cross section of the samples was polished and the final surface roughness was about 0.05 μm .

Micrindentation experiments were performed using a Micro-Tribometer, produced by the Center for Tribology (California, USA). For the present study, a cone-shaped tungsten carbide indenter with a tip radius of 0.2 mm and tip angle of 30° was used. The indentation tests were performed on the sample cross-section at steel side near the interface at a distance of 30–80 μm as shown in Fig. 3. During indentation, the load increased linearly from 0 to 30 N at a speed of 0.013 N/s. During the test, the normal load, lateral force and time were recorded. The indentation position was determined using an optical microscope. The critical load corresponding to interfacial debonding was determined by averaging at least five measurements.

3. Determination of the interfacial bond strength

Typical normal load (L)–time curve and lateral force (F_x)–time curve are illustrated in Fig. 4. As shown, when

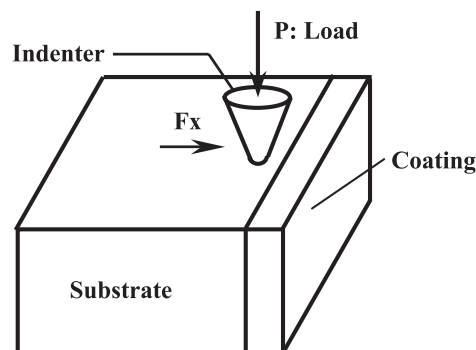


Fig. 3. Schematic illustration of the indentation test.

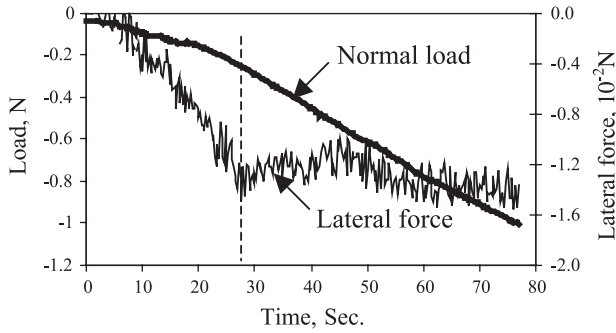


Fig. 4. Typical changes in load and lateral force vs. time for the nanostructured coating at distance of 40 μm from interface.

the normal load was increased, the lateral force changed correspondingly. At the beginning of indentation, the absolute value of F_x increased gradually until the normal load reached a certain value, and then the absolute value of the lateral force decreased. Such a change corresponded to a change in slope sign of the F_x-t curve, indicating the occurrence of interfacial debonding as demonstrated in Refs. [14,15]. An example of a resultant interfacial crack is shown in Fig. 5.

As mentioned above, the reason for the occurrence of lateral force is the asymmetric constraint on the indenter. When the stress at the interface was larger than the interfacial bond strength, debonding initiated at the interface. As a result, the asymmetric constraint changed and this resulted in a change in sign of lateral force slope. The corresponding normal load is the critical load (F_c) at interfacial debonding.

The critical loads corresponding to the interfacial debonding at different indentation positions for both Metco 130 and nanostructured coatings are shown in Fig. 6. One can see that when indentation was applied near the interface, a smaller critical load is required to cause the interfacial debonding. Compared to the Metco 130 coating, the nanocoating needed a higher critical load to cause interfacial debonding at the similar indentation position. This means that the nanocoating had higher interfacial bond strength.

To determine the local interfacial stress distribution for calculating the interfacial bond strength, a finite element model was employed to analyze the interfacial stress that

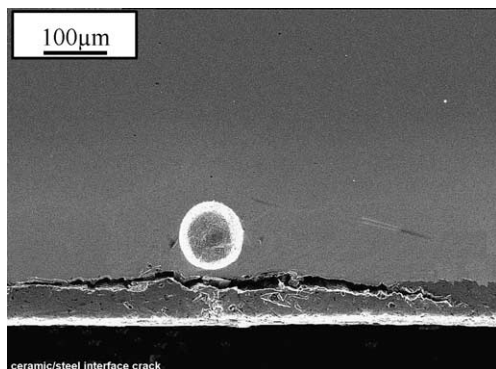


Fig. 5. Cracking at interface caused by indentation.

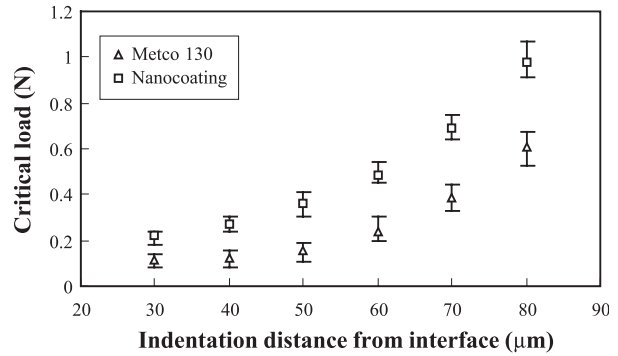


Fig. 6. The critical loads vs. indentation distance from interface for the coatings.

corresponded to the measured critical load (F_c). The FEM analysis was made using ANSYS (version 7.0) software. All parameters used for the FEM analysis had the same values as those for the indentation experiment, such as the geometry and location of indenter and material properties.

The sample substrate was modeled using isotropic eight-node solid elements with elastic–plastic properties, while the ceramic coating was fully elastic. The mesh near indenter and interface was refined to adequately reflect the stress gradient with sufficient accuracy. The indenter was assumed to be a nondeformable body. Mechanical properties of the substrate and coatings are given in Table 1. The bottom boundary of a specimen was constrained in all directions. Load was applied on the indenter until the critical load was reached. Using this model, the stress distribution at interface was calculated.

Interfacial debonding generally occurs at free edge of interface, where the singularity could exist, as demonstrated in literature [20–22]. This may make the calculated stress at a particular point in the vicinity of the free edge meaningless. Thus, an average stress approach was adopted here. The average of stress component σ_{ij} is defined as [23,24]:

$$\bar{\sigma}_{ij} = \frac{1}{x_{ave}} \int_0^{x_{ave}} \sigma_{ij} dx \quad (1)$$

where x_{ave} is a characteristic length along the interface, starting at the free edge, over which the integration is calculated. x_{ave} is treated here as an unknown parameter.

To determine the interfacial bond strength, a Quadratic Delamination Criterion [16] was adopted. This criterion takes into account both normal and shear stresses at the interface. The interfacial failure criterion between a coating

Table 1
Mechanical characteristics of involved materials

Materials	Young's modulus	Poisson's ratio	Yield stress	Tangential modulus
	E (GPa)	ν	σ_y (MPa)	E_t (GPa)
Carbon steel	200	0.25	540	10
Metco 130 coating	168.8	0.23	–	–
Nanocoating	158.2	0.23	–	–

Table 2
Interfacial bond strength determined using the lateral-force indentation method

Material	Tensile strength (MPa)	Shear strength (MPa)	x_{ave} (mm)	Coefficient of variation (CV) (%)
Metco 130 coating	26.2	11.23	0.121	5.66
Nanocoating	44.01	29.45	0.120	3.94

and a substrate is defined as

$$\left(\frac{\bar{\sigma}_{yy}}{Z}\right)^2 + \left(\frac{\bar{\sigma}_{yx}}{S}\right)^2 = 1 \quad (2)$$

where Z and S are the normal and shear interfacial bond strengths, respectively. $\bar{\sigma}_{yy}$ and $\bar{\sigma}_{yx}$ are respective average normal and shear stresses over the average length x_{ave} . This criterion was used for the present calculation; the three unknowns, Z , S , and x_{ave} need to be determined.

In order to determine Z , S , and x_{ave} , at least three indentation tests are needed. In this work, we performed five tests at different positions for a particular coating to find corresponding critical loads at interfacial debond. The following trial-and-error procedure was used to determine Z , S , and x_{ave} [16]. For each given trial set (Z , S , x_{ave}), the predicted critical load could be obtained by finite element analysis. When Eq. (2) is satisfied, the corresponding applied load is considered as the critical load, $Lc(i)$ ($i=1, 2, \dots, n$), where i represents each indentation position. The predicted critical load ($Lc(i)$) is then compared to experimentally determined critical load ($Le(i)$) using a ratio $Q(i)=Lc(i)/Le(i)$. The variation of coefficient, CV, is defined as

$$CV = \frac{\sqrt{\frac{1}{n-1} \sum (Q(i) - \bar{Q})^2}}{\bar{Q}} \quad (3)$$

where \bar{Q} is the mean value of $Q(i)$. The best-fit set (Z , S , x_{ave}) could be determined by giving a mean value $\bar{Q}=1$ while maintaining the minimum CV. Using this approach, we determined interfacial bond strengths for both the coatings, which are tabulated in Table 2.

4. Comparison of the results obtained using different methods

The result of the lateral force measurements (Table 2) indicates that the nanostructured coating has higher tensile and shear interfacial bond strengths, 44.01 and 29.45 MPa, than the commercial Metco 130 coating whose corresponding strengths are 26.2 and 11.23 MPa, respectively. The bond strength of the coatings was also measured using a modified ASTM direct pull-off test [19], in which a coated sample is glued to another bulk material and a tensile stress is applied to cause interfacial debonding. The maximum

stress at interfacial debond is the bond strength. Result of the pull-off test is given in Table 3 [19]. The results obtained using these two different methods are consistent. It is worth noting that the microindentation method yields slightly higher values than those from the pull-off test. As a matter of fact, due to the difference in mechanical properties between the coating and the substrate, normal stress and shear stress coexist at interface even under a uniaxial tension load. Therefore, it is not accurate or adequate to quantitatively evaluate interfacial failure using a pure tension test. Because the multi-axial stress state at interface has been taken into account, the lateral force microindentation should provide information that is closer to reality.

Another reason for higher interfacial bond strength determined using the microindentation method is that some defects such as microvoids or microcracks could be introduced at the interface during coating fabrication, sample cutting, and preparation. These defects may act as stress raisers, which facilitate interfacial delamination. Because the pull-off test only provides information on the overall performance of an interface, the stress concentration could result in interfacial failure under a smaller load than expected. For microindentation test, we also treat the defects as one of interfacial microstructural features. In this case, the influence of microvoids or microcracks is, however, smaller, because of the lower probability of existence of the microdefects in a local area where microindentation test is performed. As a result, the determined bond strength should be higher. If microindentation test is performed in a defect-free region, the determined bond strength will be the intrinsic interfacial bond without influence from the interfacial defects.

It was demonstrated that the nanostructured coating had a higher interfacial bond than the Metco 130 coating. The commercial Metco 130 coating is a typical plasma-sprayed coating. Microcracks were observed at its interface [18]. In the case of the nanocoating, two different interfacial zones existed, one was similar to that observed in Metco 130 coating with microcracks, the other was a partially melted zone as illustrated in Fig. 2, which is believed to be highly adherent to the substrate [18]. However, investigation of the mechanism responsible for higher interfacial bond of the nanostructured coating is beyond the scope of the present study.

From the above discussion, one might draw the conclusion that the lateral force-sensing microindentation technique can provide information on the local interfacial bond strength, including both normal and shear strength components. This technique is therefore not only useful to

Table 3
Pull-off test results [19]

Material	Tensile strength (MPa)	Coefficient of variation (CV) (%)
Metco 130	16.65	5.17
Nanocoating	39.30	3.95

evaluation of interfacial bond strength but also suitable for fundamental investigation of defects' influences on interfacial strength if microindentation tests are performed in selected regions where interfacial defects, impurity segregation, and precipitates are present. Because the indentation can be carried out on both micro-level and nano-level, this technique would be effective for characterization and evaluation of a wide range of interfaces, including those in composites, coatings, and thin films.

5. Conclusions

A newly developed lateral force-sensing microindentation technique was applied to evaluate interfacial bond strengths of regular and nanostructured $\text{Al}_2\text{O}_3/\text{TiO}_2$ coatings. Results of the test were compared to those obtained from a pull-off test. It was demonstrated that results of these two types of test were consistent. However, the interfacial bond strengths determined using the microindentation technique were higher than those from the pull-off test. Such difference could be attributed to the fact that what the microindentation test determined was closer to the intrinsic interfacial bond strength while the pull-off test only gave the average interfacial bond strength that was affected by interfacial defects such as microcracks. Furthermore, the latter did not take account of the possible effect of singularity at free edge where the influence of shear stress might also exist, which could negatively affect the accuracy of the test. This study has also demonstrated that the lateral force-sensing microindentation technique is effective and feasible not only for evaluation interfacial bond strength but also suitable for fundamental investigation of effects of interfacial defects on the interfacial strength for a variety of interfaces in composites, coatings, and thin films.

Acknowledgements

The financial support of this work by ASRA (Alberta Science and Research Associate) and NSERC (National Science and Engineering Council of Canada) is gratefully

acknowledged. The authors also would like to thank Dr. Y. Wang for providing the coating samples.

References

- [1] X.Q. Ma, F. Borit, V. Guipont, M. Jeandin, *Journal of Advanced Materials* 34 (2002) 52.
- [2] Y.Z. Yang, Z.Y. Liu, C.P. Luo, Yu.Z. Chuang, *Surface and Coatings Technology* 89 (1997) 97.
- [3] G. Burkle, F. Banhart, A. Sagel, C. Wanke, G. Croopnick, H.J. Fecht, *Materials Science Forum* 386–388 (2002) 571.
- [4] R. Beydon, G. Bernhart, Y. Segui, *Surface and Coatings Technology* 126 (2000) 39.
- [5] J.Y. Sener, D.F. Van, F. Delannay, *Journal of Adhesion Science and Technology* 15 (2001) 1165.
- [6] T. Lux, *Surface and Coatings Technology* 133–134 (2000) 425.
- [7] D. Chicot, P. Démarécaux, J. Lesage, *Thin Solid Films* 283 (1996) 151.
- [8] A.G. Evans, *Adhesion Measurement of Films and Coatings* 2 (2001) 1.
- [9] H. Ollendorf, D. Schneider, *Surface and Coatings Technology* 113 (1999) 86.
- [10] M. Toparli, S. Sasaki, *Philosophical Magazine*. A 82 (2002) 2191.
- [11] P.H. Demarecaux, D. Chicot, J. Lesage, *Journal of Materials Science Letters* 15 (1996) 1377.
- [12] J. Bystrzycki, J. Paszula, R. Rrebinski, *Journal of Materials Science* 29 (1994) 6221.
- [13] V. Gupta, J. Yuan, *Journal of Applied Physics* 74 (1993) 2397.
- [14] D.Y. Li, *Materials Science Forum* 426–432 (2003) 2053.
- [15] H. Zhang, Q. Chen, D.Y. Li, *Acta Materialia* 52 (2004) 2037.
- [16] J.C. Brewer, P.A. Lagace, *Journal of Composite Materials* 11 (1988) 1141.
- [17] Y. Wang, S. Jiang, M. Wang, S. Wang, T.D. Xiao, P.R. Strutt, *Wear* 237 (2000) 176.
- [18] P. Bansal, N.P. Padture, A. Vasiliev, *Acta Materialia* 51 (2003) 2959.
- [19] E.H. Jordan, M. Gell, Y.H. Sohn, D. Goberman, L. Shaw, S. Jiang, M. Wang, T.D. Xiao, Y. Wang, P. Strutt, *Materials Science and Engineering A301* (2001) 80.
- [20] D. Munz, Y.Y. Yang, *Journal of the European Ceramic Society* 13 (1994) 453.
- [21] M.A. Sckuhr, A. Brueckner-foit, D. Munz, Y.Y. Yang, *International Journal of Fracture* 77 (1996) 263.
- [22] A.R. Akisanya, *International Journal of Solids and Structures* 34 (1997) 1645.
- [23] R.Y. Kim, S.R. Soni, *Journal of Composite Materials* 18 (1984) 70.
- [24] S. Yi, L.X. Shen, J.K. Kim, C.Y. Yue, *Journal of Adhesion Science and Technology* 14 (2000) 93.